Contribution from the Department of Medicinal Chemistry, Hiroshima University School of Medicine, Kasumi 1-2-3, Minami-ku, Hiroshima 734, Japan, and Faculty of Pharmaceutical Sciences, University of Tokyo, Hongo, Bunkyo-ku, Tokyo 113, Japan

First X-ray Crystal Structures of Nickel(II)-Oxocyclam Complexes. Effects of the Deprotonated Amide and of an Intramolecular Pendant Pyridine on the Cyclam Ligand Field

Eiichi Kimura,*† Tohru Koike,† Hiroko Nada,† and Yoichi Iitaka‡

Received September 23, 1987

The nickel(II) complex $Ni^{II}H_{-1}L$ (**3b**) of a 14-membered macrocyclic tetraamine containing a deprotonated amide (oxocyclam) and bearing a phenyl pendant (**1b**) remains low spin in both the solid state and aqueous solution. On the other hand, the nickel(II) complex $Ni^{II}H_{-1}L$ (**5**) of oxocyclam with a pyridyl pendant (**1c**) is always high spin. The X-ray crystal structures of **3b** and **5** have been determined to find the effects of the deprotonated amide and of the pendant pyridine on the cyclam ligand field. The crystals of **3b** (as the perchlorate salt), $C_{16}H_{25}N_4ONiClO_4 \cdot H_2O$, are monoclinic, space group $P2_1$, with two molecules in the unit cell of dimensions a = 12.019 (5) Å, b = 8.915 (4) Å, c = 10.209 (5) Å, and β = 110.95 (5)°. Crystals of **5** (as the perchlorate salt), $C_{15}H_{24}N_5ONiClO_4 \cdot 2H_2O$, are triclinic, space group $P\bar{1}$, with two molecules in the unit cell of dimensions a = 11.669 (6) Å, b = 11.388 (6) Å, c = 8.535 (5) Å, α = 110.51 (6)°, β = 90.44 (5)°, and γ = 96.37 (6)°. These structures were solved by the heavy-atom method and refined by block-diagonal least-squares calculations: for **3b**, R = 0.044 for 2005 independent reflections, and for **5**, R = 0.060 for 4014 independent reflections. The effects of amide incorporation in place of the NH of cyclam is well demonstrated by comparison with cyclam congeners. The deprotonated oxocyclam can stretch its ring size distinctively with the axial pendant donor. The pH-metric titrations of **3b** and **5** have determined complexation constants (log $([Ni^{II}H_{-1}L]a_{H^+}/[Ni^{II}][L])$ at 35 °C, I = 0.1 ($NaClO_4$)) of 6.3 ± 0.3 and 8.2 ± 0.3, respectively.

Macrocyclic tetraamine (N_4) ring size and the spin state of the encapsulated Ni^{II} are closely correlated.[1-3] The smaller [12]aneN$_4$ cavity fits the smaller low-spin Ni^{II}, while the larger [15]aneN$_4$ fits the larger high-spin Ni^{II}. With the intermediate [14]aneN$_4$ (cyclam), low-spin Ni^{II} (71%) and high-spin Ni^{II} (29%) equilibrate in aqueous solution at 25 °C.[3] However, it is octahedral, high-spin Ni^{II} complexes that most often precipitate out with two axial ligands, while few square-planar, low-spin Ni^{II} complexes are isolated.[4,5]

Earlier, we found that in aqueous solution oxocyclam (**1a**)[6,7] and dioxocyclam (**2**)[7-9] yield almost exclusively the low-spin Ni^{II} complexes $Ni^{II}H_{-1}L$ (**3a**) and $Ni^{II}H_{-2}L$ (**4**) with concomitant dissociation of their amide protons. We postulated that the in-plane cyclam cavity may be constricted by substitution of an amine for an imide anion, which would raise the $d_{x^2-y^2}$ energy level so as to destabilize the high-spin state of Ni^{II}. However, there had been no information on the crystal structure of those Ni^{II} oxocyclam complexes.

Recently, we have succeeded in introducing a series of pendants R into oxocyclams **1** using a newly developed method.[10-15] Thus, we finally obtained good crystals (as the perchlorate salt) of the low-spin Ni^{II} oxocyclam complex **3b** having R = phenyl group. Moreover, R groups can be donor ligands. These donor atoms are favorably positioned so as to be just atop the macrocyclic cavity. Hence, interest arose as to whether such pendant donor ligand fields can perturb the oxocyclam in-plane ligand field so as to affect the spin state of Ni^{II}. When the pendants R are phenolate[10-12] and imidazole,[14] Ni^{II} is found to remain low spin in **6** or to have a mixed spin state in **7** in aqueous solution (see Table III); i.e., those pendants do not have sufficient interaction with Ni^{II}. In contrast, with the pyridyl-pendant homologue[13] Ni^{II} is almost completely high spin (pink) in aqueous solution. We have obtained crystalline **5** (as the perchlorate salt) and subjected it to X-ray crystal structure analysis, along with **3b**, the Ni^{II} complex of the phenyl-pendant homologue. Comparison of their structural parameters reveals well the effects of the pendant pyridyl coordination. Moreover, comparison of **3b** with the high-spin Ni^{II}-cyclam complex **8**[4,5] and the high-spin Ni^{II}-pyridyl-pendant

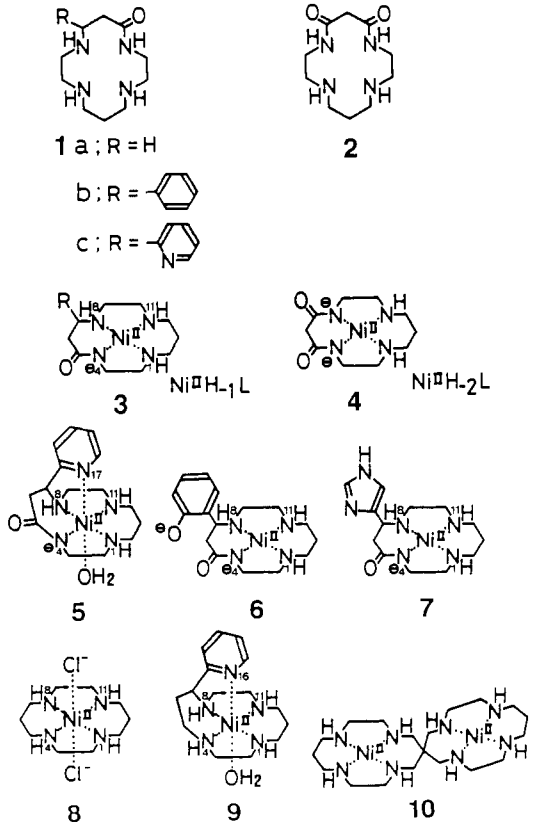

† Hiroshima University School of Medicine.
‡ University of Tokyo.

(1) Martin, L. Y.; DeHayes, L. J.; Zompa, L. J.; Busch, D. H. *J. Am. Chem. Soc.* **1974**, *96*, 4046-4048.
(2) Martin, L. Y.; Sperati, C. R.; Busch, D. H. *J. Am. Chem. Soc.* **1977**, *99*, 2968-2981.
(3) Fabbrizzi, L.; Micheloni, M.; Paoletti, P. *Inorg. Chem.* **1980**, *19*, 535-538.
(4) Bosnich, B.; Mason, R.; Pauling, P. J.; Robertson, G. B.; Tobe, M. L. *Chem. Commun.* **1965**, 97-98.
(5) Thöm, V. J.; Fox, C. C.; Boeyens, J. C. A.; Hancock, R. D. *J. Am. Chem. Soc.* **1984**, *106*, 5947-5955.
(6) Kimura, E. *J. Coord. Chem.* **1986**, *15*, 1-22.
(7) Kimura, E.; Koike, T.; Machida, R.; Nagai, R.; Kodama, M. *Inorg. Chem.* **1984**, *23*, 4181-4188.
(8) Kodama, M.; Kimura, E. *J. Chem. Soc., Dalton Trans.* **1979**, 325-329.
(9) Kodama, M.; Kimura, E. *J. Chem. Soc., Dalton Trans.* **1981**, 694-700.
(10) Kimura, E.; Koike, T.; Takahashi, M. *J. Chem. Soc., Chem. Commun.* **1985**, 385-386.
(11) Iitaka, Y.; Koike, T.; Kimura, E. *Inorg. Chem.* **1986**, *25*, 402-404.
(12) Kimura, E.; Koike, T.; Uenishi, K.; Hediger, M.; Kuramoto, M.; Joko, S.; Arai, Y.; Kodama, M.; Iitaka, Y. *Inorg. Chem.* **1987**, *26*, 2975-2983.
(13) Kimura, E.; Koike, T.; Nada, H.; Iitaka, Y. *J. Chem. Soc., Chem. Commun.* **1986**, 1322-1323.
(14) Kimura, E.; Shionoya, M.; Mita, T.; Iitaka, Y. *J. Chem. Soc., Chem. Commun.* **1987**, 1712-1714.
(15) Kimura, E. *Pure Appl. Chem.* **1986**, *58*, 1461-1466.

0020-1669/88/1327-1036$01.50/0

Table I. Protonation Constants and Ni^{II} Complex Formation Constants for Oxocyclams **1** at 35 °C and I = 0.1 ($NaClO_4$)

	phenyl-pendant oxocyclam **1b**	pyridyl-pendant oxocyclam **1c**
pK_1	10.53 ± 0.03	10.54 ± 0.03
pK_2	6.08 ± 0.02	6.06 ± 0.02
pK_3	2.5 ± 0.1	3.55 ± 0.05
pK_4		<2
log $K_{Ni^{II}H_{-1}L}$[a]	6.3 ± 0.3	8.2 ± 0.3

[a] $K_{Ni^{II}H_{-1}L} = [Ni^{II}H_{-1}L]a_{H^+}/[Ni^{II}][L]$.

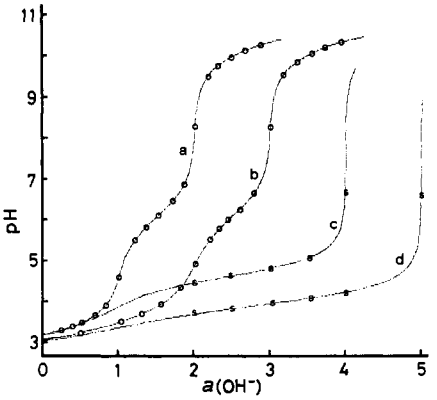

Figure 1. Calculated titration curves with the values of pK_a and $K_{Ni^{II}H_{-1}L}$ obtained from experimental values (o and s) for (a) 1.00 mM **1b** + 3.00 mM $HClO_4$, (b) 1.00 mM **1c** + 4 mM $HClO_4$, (c) solution as in (a) + 1.00 mM $NiSO_4$, and (d) solution as in (b) + 1.00 mM $NiSO_4$ at 35 °C and I = 0.1 ($NaClO_4$).

cyclam complex **9**[13] sheds light on the structural effects of the deprotonated amide coordination.

Experimental Section

General Methods. All the starting materials were obtained commercially and were used without further purification. Visible spectra were recorded on a Hitachi U-3200 spectrophotometer at 25.0 ± 0.1 °C and I = 0.1 M ($NaClO_4$) using matched quartz cells of 10- or 50-mm path length, IR spectra were obtained on a Shimazu IR-408 spectrophotometer, and ^1H NMR spectra were recorded and magnetic measurements were performed (by the Evans method[16]) on a Hitachi R-40 high-resolution NMR spectrometer (90 MHz, 35 °C).

Synthesis of the Pendant–Oxocyclam Compounds 1b and 1c. 5-Oxo-7-phenyl-1,4,8,11-tetraazacyclotetradecane (**1b**)[12] and 5-oxo-7-(2-pyridyl)-1,4,8,11-tetraazatetradecane (**1c**)[13] were synthesized from the corresponding α,β-unsaturated esters and 1,9-diamino-3,7-diazanonane by our newly developed method.[15]

Potentiometric Titrations. The preparation of the test solutions and the calibration of the electrode system were described earlier in detail.[12] The temperature was maintained at 35.00 ± 0.05 °C, and the ionic strength was adjusted to 0.10 M with $NaClO_4$ (pK_w = 13.68 and f_{H^+} = 0.835[17]). Ni^{II} complex formation was not rapidly attained during any part of the titration. Consequently, each titration point was obtained from a separately prepared solution to which was added the desired quantity of 0.10 M NaOH solution. The solutions were stored under argon for 3 days at 35 °C for sufficient equilibration, and then their pHs were measured. The titration data were treated by a desktop-computer-aided Schwarzenbach method.[7] The pK_a values and Ni^{II} complex formation constants are given in Table I. Calculated titration curves are shown in Figure 1 with the values of pK_a and $K_{Ni^{II}H_{-1}L}$ obtained from experimental values.

Crystallographic Study. A yellow crystal of dimensions 0.1 × 0.3 × 0.4 mm^3 of **3b** and a violet crystal of dimensions 0.2 × 0.3 × 0.3 mm^3 of **5** were used for data collection at room temperature. The lattice parameters and intensity data were measured on a Philips PW-1100 automatic four-circle diffractometer by using graphite-monochromated Cu Kα radiation. Crystal data and data collection parameters are displayed in Table II. These structures were solved by the heavy-atom method and refined by the block-diagonal-matrix least-squares method. The hydrogen atoms were located on the difference electron-density map, and their positions were at first regularized by the standard bond lengths and bond angles and then included in the least-squares refinement with isotropic temperature factors. The final R values for **3b** and **5** are 0.044 and 0.060, respectively.

Table II. Crystal Data and Data Collection Symmary

	3b	**5**
formula	$C_{16}H_{25}N_4ONiClO_4 \cdot H_2O$	$C_{15}H_{24}N_5ONiClO_4 \cdot 2H_2O$
fw	465.6	484.5
cryst syst	monoclinic	triclinic
space group	$P2_1$	$P\bar{1}$
cell dimens		
a, Å	12.019 (5)	11.669 (6)
b, Å	8.915 (4)	11.388 (6)
c, Å	10.209 (5)	8.535 (5)
α, deg	90.00	110.51 (6)
β, deg	110.95 (5)	90.44 (5)
γ, deg	90.00	96.37 (6)
V, Å^3	1022	1054
Z	2	2
calcd density, g cm^{-3}	1.513	1.527
cryst color	yellow	violet
cryst dimens, mm^3	0.1 × 0.3 × 0.4	0.2 × 0.3 × 0.3
radiation	Cu Kα (graphite monochromated)	
μ, cm^{-1}	29.3	29.1
2θ range, deg	6–156	
scan speed, deg min^{-1}	6	
phasing	heavy-atom method	
no. of measd rflns	2272	4368
no. of indep rflns ($I > 2\sigma(I)$)	2005	4014
refinement	block-diagonal-matrix least-squares method	
final R	0.044	0.060
no. of refined atoms	28 (anisotropic) + 25 H (isotropic)	29 (anisotropic) + 28 H (isotropic)

Table III. Visible Absorption Maxima (at 25 °C, pH 7.0, and I = 0.1 ($NaClO_4$)) and Magnetic Susceptibilities (μ_{eff} at 35 °C and I = 0.1 ($NaClO_4$)) of Ni^{II}–Oxocyclam and -Cyclam Complexes

Ni^{II} complex	λ_{max}, nm (ϵ)	μ_{eff}, μ_B	Ni^{II} complex	λ_{max}, nm (ϵ)	μ_{eff}, μ_B
3b	448 (80)	<0.3	**7**[b]	447 (60)	1.54
5	494 (13)	2.90	**8**[b]	450 (70)	2.35
6[a]	447 (80)	<0.3	**9**	523 (8)	2.88

[a] Phenolate form at pH 10.5. [b] Mixed-spin Ni^{II} complexes in aqueous solution.

Preparation of the Ni^{II} Complexes 3b and 5. The pendant–oxocyclam (**1b** and **1c**, 0.5 mmol) and $NiSO_4$ (0.5 mmol) were dissolved in 50 mL of 0.1 M $NaClO_4$ aqueous solution at 50 °C, and the mixture was adjusted to pH 7 with 0.1 M NaOH solution. The resulting solutions were filtered, and the filtrates were allowed to stand for 2 weeks at room temperature. The yellow crystals of **3b** and the violet crystals of **5** were obtained in ca. 50% yield. Anal. Calcd for $C_{16}H_{25}N_4ONiClO_4 \cdot H_2O$, **3b**$(ClO_4) \cdot H_2O$: C, 41.28; H, 5.85; N, 12.04. Found: C, 41.14; H, 5.79; N, 12.04. Anal. Calcd for $C_{15}H_{24}N_5ONiClO_4 \cdot 2H_2O$, **5**$(ClO_4) \cdot 2H_2O$: C, 37.18; H, 5.82; N, 14.15. Found: C, 37.38; H, 5.81; N, 14.34. IR (KBr; $\nu_{C=O}$): 1550 cm^{-1} for **3b** and 1580 cm^{-1} for **5**. Their visible absorption maxima and magnetic susceptibilities in aqueous solution are summarized in comparison with those data for relevant complexes in Table III.

Results and Discussion

Oxocyclams 1b and 1c and Complexation with Nickel(II). The analogous pK_{1-3} values for **1b** and **1c** suggest that those values are for three =NH groups in the macrocyclic skeletons. Thus, the pyridyl N of **1c** has an unusually low pK_a value (<2) under the strong influence of the proximate triprotonated N_4 ring.

The $Ni^{II}H_{-1}L$ (**3b** and **5**) formations were shown by the pH-metric titration of $L \cdot 3H^+$ (for **3b**) and $L \cdot 4H^+$ (for **5**) in the presence of 1 equiv of $NiSO_4$. The titration curves (Figure 1c,d) were obtained by using independent preparations of variably neutralized test solutions, since 3 days was required for equilibration. The smooth (i.e. no break) curves until a = 4 (for **3b**)

(16) Evans, D. F. *J. Chem. Soc.* **1959**, 2003–2005.
(17) *Kagaku Binran*, 3rd ed.; Chemical Society of Japan: Tokyo, 1984; Vol. II.

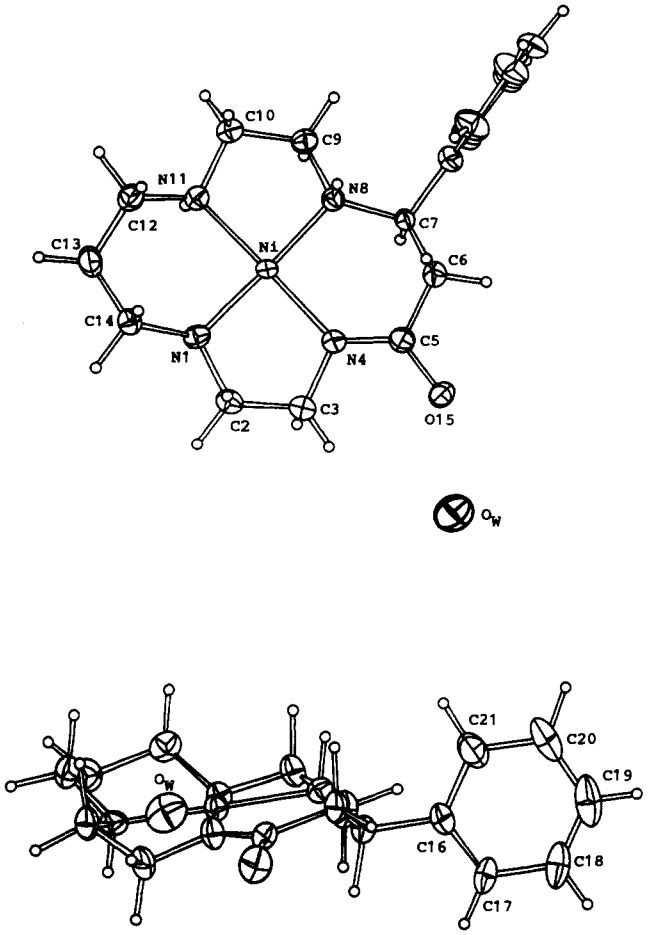

Figure 2. ORTEP drawings of complex **3b**$(ClO_4)\cdot H_2O$: top view and side-on view. The perchlorate is omitted for clarity. Atoms are drawn with 30% probability ellipsoids.

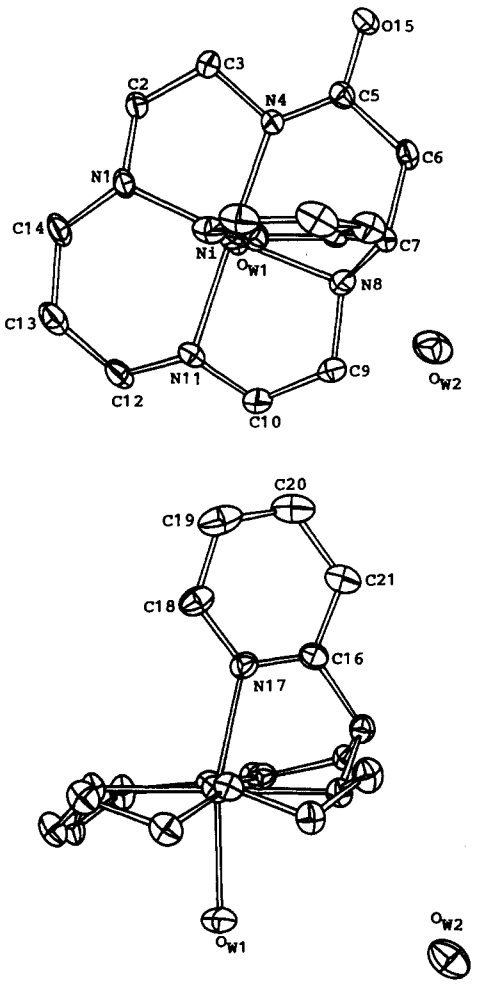

Figure 3. ORTEP drawings of complex **5**$(ClO_4)\cdot 2H_2O$: top view and side-on view. Atoms are drawn with 30% probability ellipsoids. The hydrogen atoms and perchlorate are omitted for clarity.

Table IV. Final Fractional Coordinates ($\times 10^4$) for the Ni^{II} Phenyl-Pendant Oxocyclam Complex **3b** with Estimated Standard Deviations in Parentheses

atom	x	y	z	B_{eq}, Å^2
Ni	1558.6 (8)	2965.1	3761.7 (9)	2.63 (0.01)
N(1)	3261 (4)	2673 (6)	4578 (5)	3.1 (0.1)
C(2)	3646 (5)	2874 (11)	6131 (6)	3.9 (0.1)
C(3)	2929 (5)	4143 (9)	6376 (6)	3.9 (0.1)
N(4)	1689 (4)	3892 (7)	5491 (5)	3.3 (0.1)
C(5)	853 (5)	4461 (8)	5895 (6)	3.2 (0.1)
C(6)	−421 (5)	4256 (8)	4988 (6)	3.3 (0.1)
C(7)	−687 (5)	4509 (7)	3418 (6)	2.8 (0.1)
N(8)	−136 (4)	3230 (6)	2898 (4)	2.7 (0.1)
C(9)	−429 (5)	3364 (8)	1341 (6)	3.5 (0.1)
C(10)	253 (5)	2131 (8)	982 (6)	3.5 (0.1)
N(11)	1509 (4)	2262 (6)	1933 (5)	3.2 (0.1)
C(12)	2184 (6)	895 (8)	1898 (7)	3.7 (0.1)
C(13)	3504 (6)	1067 (9)	2703 (8)	4.2 (0.1)
C(14)	3778 (6)	1244 (9)	4271 (7)	4.3 (0.1)
O(15)	1091 (4)	5230 (6)	7019 (4)	4.4 (0.1)
C(16)	−2001 (5)	4680 (8)	2578 (6)	3.3 (0.1)
C(17)	−2399 (6)	5895 (9)	1694 (6)	4.0 (0.1)
C(18)	−3596 (6)	6057 (11)	895 (7)	5.5 (0.2)
C(19)	−4398 (7)	5076 (14)	955 (9)	7.2 (0.2)
C(20)	−4024 (7)	3814 (13)	1842 (10)	7.1 (0.2)
C(21)	−2822 (6)	3639 (11)	2660 (9)	5.6 (0.2)
O(W)	2186 (5)	4284 (7)	9835 (5)	6.0 (0.1)
Cl	2711 (2)	6646 (2)	2804 (2)	4.5 (0.0)
O(1Cl)	1549 (6)	6327 (15)	2577 (8)	12.0 (0.2)
O(2Cl)	2774 (6)	7409 (7)	1593 (6)	7.0 (0.1)
O(3Cl)	3409 (7)	5298 (7)	2973 (7)	8.3 (0.2)
O(4Cl)	3266 (6)	7595 (8)	3991 (6)	7.6 (0.1)

and $a = 5$ (for **5**) indicate that the dissociation of the amide proton is simultaneous with complexation. From the analysis of the titration data (indicated as s in Figure 1c,d), the 1:1 Ni^{II} complexation constants $K_{Ni^{II}H_{-1}L}$ were determined. Evidently the pendant-pyridyl coordination contributes to the Ni^{II} complex stability.

The d–d absorption bands are in contrast for yellow **3b** and pink **5**, representing typical low-spin and high-spin Ni^{II} complexes, respectively. Addition of pyridine (up to 10 equiv) to **3a** or **3b** aqueous solutions at pH 8 and 25 °C does not change those yellow d–d bands, illustrating the significance of the pendant pyridine. Similar visible absorptions are reported for Ni^{II}–cyclam complexes (see Table III). The magnetic susceptibilities measured in aqueous solutions by the Evans method indicate nearly 100% low-spin nickel for **3b** and **6**, nearly 100% high-spin nickel for **5**, and mixed-spin nickel for **7**.

Crystal Structures of 3b and 5. The X-ray crystal structures for **3b** and **5** are the first ones for oxocyclam complexes, which are shown in Figures 2 and3, respectively, by ORTEP drawings with 30% probability thermal ellipsoids. The atomic positional parameters are given in Tables IV and V. Selected interatomic distances and bond angles are listed in comparison with those of the relevant complexes **8** and **9** with the same numbering in Tables VI and VII. Short hydrogen bond distances are presented in Table VIII.

The observed Ni–N bond distances support the low-spin Ni^{II} for **3b** and high-spin Ni^{II} for **5**. Another interesting finding from the X-ray study is that the oxocyclam ring is not always constrictive. Like the cyclam ring it is rather elastic and can be stretched to accommodate the central metal size.

The four-N-coordinate, square-planar geometry for the low-spin Ni^{II}–oxocyclam complex **3b** is evident (see Figure 2). The atoms N(1), N(4), N(8), and N(11) in the cyclam skeleton are coplanar,

Table V. Final Fractional Coordinates ($\times 10^4$) for the Ni^{II} Pyridyl-Pendant Oxocyclam Complex **5** with Estimated Standard Deviations in Parentheses

atom	*x*	*y*	*z*	B_{eq}, Å^2
Ni	2912.5 (5)	3140.9 (5)	1968.9 (7)	2.44 (0.01)
N(1)	1351 (3)	3868 (3)	2311 (4)	2.9 (0.1)
C(2)	1563 (4)	5032 (4)	3823 (5)	3.4 (0.1)
C(3)	2216 (4)	4771 (4)	5199 (5)	3.4 (0.1)
N(4)	3156 (3)	4022 (3)	4467 (4)	2.7 (0.0)
C(5)	3977 (3)	3955 (3)	5467 (5)	2.7 (0.1)
C(6)	4872 (3)	3055 (4)	4754 (5)	3.0 (0.1)
C(7)	4595 (3)	1958 (3)	3064 (5)	2.9 (0.1)
N(8)	4497 (3)	2466 (3)	1700 (4)	2.8 (0.8)
C(9)	4490 (4)	1521 (4)	−19 (5)	3.6 (0.1)
C(10)	3826 (4)	1954 (4)	−1211 (5)	3.6 (0.1)
N(11)	2656 (3)	2156 (3)	−597 (4)	3.0 (0.1)
C(12)	1949 (4)	2709 (4)	−1552 (5)	3.9 (0.1)
C(13)	795 (4)	2977 (4)	−768 (6)	4.1 (0.1)
C(14)	850 (4)	4119 (4)	863 (5)	3.6 (0.1)
O(15)	4120 (2)	4598 (3)	7038 (3)	3.4 (0.0)
C(16)	3475 (3)	1145 (3)	3081 (5)	2.9 (0.1)
N(17)	2516 (3)	1450 (3)	2522 (4)	2.9 (0.1)
C(18)	1501 (4)	803 (4)	2601 (6)	3.9 (0.1)
C(19)	1403 (5)	−154 (5)	3239 (6)	5.1 (0.1)
C(20)	2379 (5)	−485 (5)	3773 (7)	5.5 (0.1)
C(21)	3447 (4)	168 (4)	3687 (6)	4.1 (0.1)
O(W1)	3721 (3)	4794 (3)	1523 (4)	3.8 (0.1)
O(W2)	3146 (4)	6171 (4)	−365 (4)	5.8 (0.1)
Cl	1750 (1)	8397 (1)	−2219 (2)	4.5 (0.0)
O(1Cl)	1312 (4)	9566 (4)	−1667 (8)	9.3 (0.1)
O(2Cl)	2689 (5)	8295 (8)	−3162 (10)	14.0 (0.2)
O(3Cl)	947 (5)	7522 (6)	−3023 (14)	22.5 (0.3)
O(4Cl)	2142 (14)	8208 (11)	−854 (11)	28.7 (0.5)

Scheme I

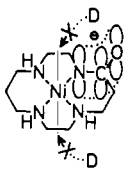

steric hindrance at axial sites
Ni^{II}–oxocyclam (**3**)

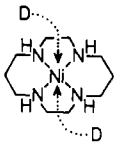

less steric hindrance
Ni^{II}–cyclam (**8**)

and the Ni^{II} ion is in this plane. As anticipated, the bond distance for Ni–N(4)(imide) is shorter at 1.905 (5) Å than those for other Ni–NH(saturated) (ca. 1.93 Å). These bonding characteristics are reminiscent of square-planar, low-spin Ni^{II}–14-membered cyclic amine–imine N_4 complexes: Ni–N(imine) and Ni–N(amine) bond distances are ~1.90 and ~1.93 Å, respectively.[18] The reported low-spin Ni^{II}–NH bond distances in the cyclam complex **10** are 1.94–1.96 Å.[19] The most common chair conformation of the cyclam ("trans III form")[5] prevails in **3b**. It thus seems that the deprotonated oxocyclam ring is not appreciably tighter than the cyclam ring for low-spin Ni^{II}. Axial coordination of D (e.g. H_2O) to Ni^{II} in the oxocyclam may be electronically and sterically hindered due to the adjacent $(N–C–O)^-$ π-electron cloud on the macrocycle, which shortens the in-plane Ni–N bonds and squeezes Ni^{II} into the low-spin configuration (Scheme I). Similarly, Ni^{II} in the cyclam ring takes a low-spin state with shortened Ni–N bond lengths of 1.94–1.96 Å, when the axial access is difficult (e.g. **10**).[19] It is to be noted that with a bulky axial ligand I^- that stays remote (3.34 Å) in Ni^{II}–cyclam the Ni–N bond lengths are also shortened to 1.94 Å.[20] On the other hand, as in the Ni^{II}–cyclam complex **8**, when axial ligands can come closer without steric hindrance, the cyclam ring is stretched to

Table VI. Comparison of Bond Distances (Å) for **3b**, **5**, **8**, and **9** with Estimated Standard Deviations in Parentheses

	3b	**5**	**8**[a]	**9**[a]
Ni–N(1)	1.931 (4)	2.065 (3)	2.050	2.058
Ni–N(4)	1.905 (5)	2.015 (3)	2.066	2.093
Ni–N(8)	1.923 (4)	2.065 (3)		2.056
Ni–N(11)	1.950 (5)	2.083 (3)		2.068
N(1)–C(2)	1.496 (8)	1.485 (4)	1.484	1.493
N(1)–C(14)	1.499 (10)	1.491 (6)	1.530	1.487
C(2)–C(3)	1.496 (12)	1.526 (7)	1.565	1.512
C(3)–N(4)	1.458 (7)	1.472 (5)	1.512	1.481
N(4)–C(5)	1.315 (9)	1.305 (5)	1.525	1.483
C(5)–C(6)	1.491 (7)	1.524 (5)	1.570	1.508
C(6)–C(7)	1.535 (9)	1.545 (5)	1.577	1.540
C(7)–N(8)	1.508 (8)	1.478 (6)		1.477
N(8)–C(9)	1.504 (7))	1.484 (5)		1.482
C(9)–C(10)	1.493 (10)	1.518 (7)		1.511
C(10)–N(11)	1.479 (7)	1.480 (6)		1.479
N(11)–C(12)	1.471 (9)	1.485 (6)		1.476
C(12)–C(13)	1.511 (9)	1.522 (7)		1.515
C(13)–C(14)	1.522 (11)	1.531 (5)		1.518
C(16)–C(21)	1.379 (11)	1.380 (7)		
C(18)–C(19)	1.319 (14)	1.372 (8)		
C(19)–C(20)	1.413 (16)	1.362 (9)		
C(20)–C(21)	1.395 (10)	1.394 (8)		
Cl–O(1Cl)	1.362 (8)	1.404 (4)		
Cl–O(2Cl)	1.473 (7)	1.355 (7)		
Cl–O(3Cl)	1.441 (8)	1.283 (6)		
Cl–O(4Cl)	1.432 (6)	1.342 (12)		
C(7)–C(16)	1.511 (7)	1.519 (5)		
C(5)–O(15)	1.278 (8)	1.282 (4)		
C(16)–C(17)	1.381 (10)			
C(17)–C(18)	1.385 (9)			
C(16)–N(17)		1.339 (5)		
N(17)–C(18)		1.339 (5)		
Ni–N(17)		2.142 (4)		2.124[b]
Ni–O(W1)		2.166 (3)		2.237
Ni–Cl			2.402	

[a] In this and in the following tables for **8** and **9**, the data are taken from the Supplemental Material of ref 4 and 13, respectively. The atomic numbers for **9** described in ref 13 are adapted to the same numbering as for **5**. [b] Bond length for Ni–N(axial pyridyl).

Scheme II

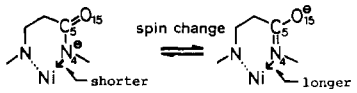

form I
favorable for
low-spin Ni^{II}

form II
favorable for
high-spin Ni^{II}

accommodate the larger high-spin Ni^{II} (the ideal strain-free high-spin Ni^{II}–N bond distance is 2.10 Å).[5]

For deprotonation of the amide group in oxocyclam complexes, the two extreme resonance forms I and II may be depicted (Scheme II). In fact, the C=O (1.278 Å) and OC—N (1.315 Å) bond distances for **3b** indicate the delocalization of the carbonyl similar to those distances (1.27 and 1.30 Å, respectively) for low-spin Ni^{II}–peptide complexes.[21]

The six-coordinate octahedral coordination for high-spin Ni^{II} in **5** is unequivocally proven by the X-ray crystal structure. The pyridine ring stands vertically above the N_4 plane to allow its nitrogen donor N(17) an axial coordination, although it is with appreciable strain, as seen from displacement from the apex of a regular pyramidal arrangement, e.g. the N(4)–Ni–N(17) angle of 85.6°. The axial Ni–N(17) bond distance of 2.141 (4) Å may be viewed as being extremely short considering the steric crowding in the oxocyclam. This intruding axial pyridyl coordination causes the following. (i) The oxocyclam ring expands, with the equatorial Ni–NH bonds (average 2.07 Å, excluding the Ni–N(imide) bond)

(18) Curtis, N. F. In *Coordination Chemistry of Macrocyclic Compounds*; Melson, G. A., Ed.; Plenum: Press: New York, 1979; 219–344.
(19) McAuley, A.; Subramanian, S.; Whitcombe, T. W. *J. Chem. Soc., Chem. Commun.* **1987**, 539–541.
(20) Prasad, L.; McAuley, A. *Acta Crystallogr., Sect. C: Cryst. Struct. Commun.* **1983**, *C39*, 1175–1177.
(21) Freeman, H. C.; Guss, J. M.; Sinclair, R. L. *J. Chem. Soc., Chem. Commun.* **1986**, 485–487.

Table VII. Comparison of Bond Angles (deg) for **3b**, **5**, **8**, and **9** with Estimated Standard Deviations in Parentheses

	3b	5	8	9
N(1)–C(2)–C(3)	106.8 (6)	110.3 (3)	106.5	108.3
N(1)–C(14)–C(13)	111.0 (6)	112.5 (4)	108.2	112.7
C(2)–N(1)–C(14)	109.2 (5)	112.0 (3)	109.8	112.5
C(2)–C(3)–N(4)	107.7 (6)	109.3 (3)	106.4	109.6
C(3)–N(4)–C(5)	118.2 (5)	118.6 (3)	109.0	112.6
N(4)–C(5)–C(6)	119.2 (6)	119.1 (3)	107.1	113.3
C(5)–C(6)–C(7)	114.5 (5)	119.3 (3)	111.6	115.9
C(6)–C(7)–N(8)	107.6 (5)	109.9 (3)		110.3
C(7)–N(8)–C(9)	110.2 (4)	115.1 (3)		114.4
C(8)–C(9)–N(10)	105.0 (5)	109.1 (3)		109.2
C(9)–C(10)–N(11)	107.6 (5)	108.6 (3)		109.0
C(10)–N(11)–C(12)	111.1 (5)	114.3 (3)		113.2
N(11)–C(12)–C(13)	112.6 (6)	111.1 (4)		111.8
C(12)–C(13)–C(14)	111.9 (6)	115.2 (4)		114.7
N(4)–C(5)–O(15)	122.5 (6)	125.8 (4)		
C(6)–C(5)–O(15)	118.3 (6)	115.2 (3)		
C(6)–C(7)–C(16)	113.1 (5)	111.7 (3)		
C(7)–C(16)–C(21)	121.5 (6)	121.5 (4)		
N(8)–C(7)–C(16)	112.1 (5)	108.8 (3)		
C(16)–C(21)–C(20)	119.9 (8)	118.5 (5)		
C(18)–C(19)–C(20)	119.2 (9)	118.9 (5)		
C(19)–C(20)–C(21)	119.8 (9)	119.3 (5)		
N(1)–Ni–N(4)	86.3 (2)	84.2 (1)	85.7	84.9
N(1)–Ni–N(11)	92.0 (2)	96.7 (1)	94.3	95.3
N(4)–Ni–N(8)	95.4 (2)	94.0 (1)		94.7
N(8)–Ni–N(11)	86.3 (2)	85.1 (1)		85.1
N(1)–Ni–O(W1)		90.8 (1)		92.8
N(4)–Ni–N(17)		85.6 (1)		89.0[a]
N(8)–Ni–N(17)		79.1 (1)		79.2[b]
N(17)–Ni–O(W1)		166.7 (1)		166.2[c]
Ni–N(17)–C(16)		109.9 (3)		
C(7)–C(16)–N(17)		116.5 (3)		
C(16)–N(17)–C(18)		118.5 (4)		
N(17)–C(18)–C(19)		122.7 (4)		
C(7)–C(16)–C(17)	119.8 (6)			
C(16)–C(17)–C(18)	120.7 (7)			
C(17)–C(18)–C(19)	121.7 (8)			

[a] Angle of N(4)–Ni–N(axial pyridyl). [b] Angle of N(8)–Ni–N(axial pyridyl). [c] Angle of N(axial pyridyl)–Ni–O(W1).

expanding to almost the same Ni–N distances (2.06 Å) as in the cyclam complex **8** (see Table VI). (ii) The Ni–N(imide) bond distance similarly lengthens from 1.905 Å in **3b** to 2.015 Å in **5**. This represents a contribution of the resonance form II for the high-spin Ni^{II} complex **5**, as compared with the contribution of form I for the low-spin Ni^{II} of **3b** (Scheme II). By use of this scheme the Ni–N^- bond lengths may be linked with the C–O and C–N bond distances, but this is not verified in the comparative

Table VIII. Short Hydrogen Bond Distances (Å) for **3b** and **5** with Estimated Deviations in Parentheses

	3b		
O(3Cl)···HN(1)^{i}[a]	2.032 (64)	O(W)···HN(11)^{iii}	2.212 (85)
O(15)···HN(8)^{ii}	1.971 (58)		
	5		
O(W2)···H′O(W1)^{i}	1.857 (66)	O(1Cl)···HN(11)^{v}	2.080 (38)
O(4Cl)···HO(W2)^{i}	1.979 (70)	O(15)···H′O(W2)^{iii}	1.964 (55)
O(15)···HO(W1)^{iv}	1.982 (44)	O(3Cl)···HN(1)^{vi}	2.231 (50)

[a] Atomic positions: (i) x, y, z; (ii) $-x, {}^1/_2 + y, 1 - z$; (iii) $x, y, 1 + z$; (iv) $1 - x, 1 - y, 1 - z$; (v) $x, 1 + y, z$; (vi) $-x, 1 - y, -z$.

X-ray study of **3b** and **5**, probably due to involvement of other factors such as intermolecular hydrogen bonds. (iii) As a consequence, the Ni^{II} spin state changes from low to high. (iv) The sixth axial coordination of H_2O is at the fairly short distance of 2.166 Å.

The fact that both low-spin and high-spin states of Ni^{II} can be accommodated within oxocyclam implies that the origin of the low-spin complex **5** is not caused by the compression by the monooxo macrocycle but is a consequence of the steric hindrance at the axial site and of correspondingly shortened Ni–N bond lengths. This explanation can be applied to the dioxocyclam complexes of low-spin Ni^{II}. Only with the intramolecular pendant donors does axial access become possible and do the in-plane Ni–N bonds lengthen, permitting the high-spin Ni^{II} complex **5**.

Comparison of the axial pyridyl bond distances for oxocyclam **5** and cyclam **9** reveals the effect of the equatorial oxo function on cyclam. The π-electron cloud of the imide anion causes the axial Ni–N(17) bond of **5** (2.142 Å) to be longer than the Ni–N(16) bond of **9** (2.124 Å). In reflection of these different axial interactions, the trans Ni–OH_2 bond distance changes from 2.166 Å for **5** to 2.237 Å for **9**. The overall cyclam ring size itself is virtually unaffected with or without the oxo group. In the visible spectra (Table I) the lower λ_{max} for the oxocyclam complex **5** (494 nm) than for the cyclam complex **9** (523 nm) indicates a stronger overall ligand field for the former oxo system.

Acknowledgment. We thank the Ministry of Education for financial assistance by a Grant-in-Aid for Special Project Research (No. 60119003).

Registry No. **1b**, 98096-22-1; **1c**, 108643-56-7; **3b**$(ClO_4)\cdot H_2O$, 112764-09-7; **5**$(ClO_4)\cdot H_2O$, 112764-12-2.

Supplementary Material Available: Listings of hydrogen atom positional parameters and of thermal parameters for **3b** and **5** (4 pages); tables of calculated and observed structure factors for the two complexes (12 pages). Ordering information is given on any current masthead page.